J|A|C|S
ARTICLES
Published on Web 10/24/2006

The Boat-Shaped Polyketide Resistoflavin Results from *Re*-Facial Central Hydroxylation of the Discoid Metabolite Resistomycin

Keishi Ishida,[†] Katja Maksimenka,[‡] Kathrin Fritzsche,[†] Kirstin Scherlach,[†] Gerhard Bringmann,*[,‡] and Christian Hertweck*[,†,§]

Contribution from the Department of Biomolecular Chemistry, Leibniz Institute for Natural Product Research and Infection Biology (HKI), Beutenbergstrasse 11a, D-07745 Jena, Institute for Organic Chemistry, University of Würzburg, Am Hubland, D-97074 Würzburg, and Friedrich-Schiller-University Jena, D-07737 Jena, Germany

Received June 27, 2006; E-mail: christian.hertweck@hki-jena.de; bringman@chemie.uni-wuerzburg.de

Abstract: Resistoflavin (**1**) is a rare boat-shaped pentacyclic polyketide metabolite of *Streptomyces resistomycificus* with marked antibacterial activity. By a series of experiments we have disclosed that the optically active molecule is derived from the discoid polyketide resistomycin (**2**) by an unusual, enantioface-differentiating hydroxylation, which leads to the capped pentacyclic ring system. In vivo and in vitro experiments unequivocally demonstrate that this reaction is catalyzed by RemO, an FAD-dependent monooxygenase. In addition, we were able to establish the absolute configuration of **1** and thus the stereochemical course of this rare enzymatic reaction by extensive computational methods. Comparison of the experimental CD spectrum with those quantum chemically calculated for (*R*)-**1** and (*S*)-**1** revealed the *R*-configuration of **1**. Consequently, the enzyme-catalyzed hydroxylation takes place from the *Re*-face of **2** with loss of aromaticity in favor of a chiral carbinol center. While other oxygenases involved in polyketide tailoring functionalize the periphery of polyphenols, RemO is unique in its ability to catalyze a central, nonperipheral hydroxylation of a fused ring system.

Introduction

Aromatic polyketides from Actinomycetes comprise a large group of metabolites, many of which are medicinally relevant.[1,2] A hallmark for their biosynthesis is the assembly of poly-β-keto chains from malonyl-CoA units by repetitive Claisen condensations. Aromatic polyketide synthases (type II PKSs) represent the core and motor of this biosynthetic machinery.[3,4] It is remarkable that the multienzyme complex utilizes only a limited number of biosynthetic building blocks and only a few basic cyclization patterns are realized in nature, as cycloaromatization of the nascent poly-β-keto intermediates generally leads to planar polyphenolic ring systems (linear, angular, discoid).[5] Consequently, the vast diversity of aromatic polyketides is largely a result of so-called tailoring reactions catalyzed by various types of transferases and oxygenases.[6] Many oxidative post-PKS enzymes catalyze intriguing ring-opening and rearrangement cascades that lead to three-dimensional structures, as impressively demonstrated in the biosynthetic pathways of enterocin,[7,8] griseorhodin,[9] gilvocarcin,[10] jadomycin,[11] chartreusin,[12] and fredericamycin.[13] Apart from such dramatic multistep reactions, a single hydroxylation may already introduce a significant twist into a planar ring system. This is clearly the case when the aromaticity of a polyphenolic system is—at least partially—lost by hydroxylation in favor of a chiral carbinol center. Such regio- and stereospecific enzymatic reactions are particularly interesting from a synthetic point of view as they cannot be emulated by the currently existing chemical reagents.

A remarkable example of a nonplanar, oxofunctionalized polyketide is the "hood"- or "boat"-shaped resistoflavin (**1**, Figure 1), a pentacyclic polyphenol with a marked inhibitory effect on macromolecule synthesis in *Bacillus subtilis*.[14] Compared to the related flat, "discoid" polyketide resistomycin (**2**), the pentacyclic ring system of **1** is clearly out of plane surmounted by the central hydroxyl moiety.

[†] HKI.
[‡] University of Würzburg.
[§] Friedrich-Schiller-University Jena.

(1) O'Hagan, D. *The Polyketide Metabolites*; Ellis Horwood: Chichester, U.K., 1991.
(2) Hertweck, C.; Luzhetskyy, A.; Rebets, Y.; Bechthold, A. *Nat. Prod. Rep.*, in press.
(3) Rawlings, B. J. *Nat. Prod. Rep.* **1999**, *16*, 425−484.
(4) Shen, B. *Top. Curr. Chem.* **2000**, *209*, 1−51.
(5) Jakobi, K.; Hertweck, C. *J. Am. Chem. Soc.* **2004**, *116*, 2298−2299.
(6) Rix, U.; Fischer, C.; Remsing, L. L.; Rohr, J. *Nat. Prod. Rep.* **2002**, *19*, 542−580.
(7) Piel, J.; Hertweck, C.; Shipley, P.; Hunt, D. S.; Newman, M. S.; Moore, B. S. *Chem. Biol.* **2000**, *7*, 943−955.
(8) Xiang, L.; Kalaitzis, J. A.; Moore, B. S. *Proc. Natl. Acad. Sci. U.S.A.* **2004**, *101*, 15609−15614.
(9) Li, A.; Piel, J. *Chem. Biol.* **2002**, *9*, 1017−1026.
(10) Fischer, C.; Lipata, F.; Rohr, J. *J. Am. Chem. Soc.* **2003**, *125*, 7818−7819.
(11) Rix, U.; Wang, C.; Chen, Y.; Lipata, F. M.; Remsing Rix, L. L.; Greenwell, L. M.; Vining, L. C.; Yang, K.; Rohr, J. *ChemBioChem* **2005**, *6*, 838−845.
(12) Xu, Z.; Jakobi, K.; Welzel, K.; Hertweck, C. *Chem. Biol.* **2005**, *12*, 579−588.
(13) Wendt-Pienkowski, E.; Huang, Y.; Zhang, J.; Li, B.; Jiang, H.; Kwon, H.; Hutchinson, C. R.; Shen, B. *J. Am. Chem. Soc.* **2005**, *127*, 16442−16452.
(14) Haupt, I.; Eckardt, K. *Z. Allg. Mikrobiol.* **1972**, *12*, 573−579.

10.1021/ja064550u CCC: $33.50

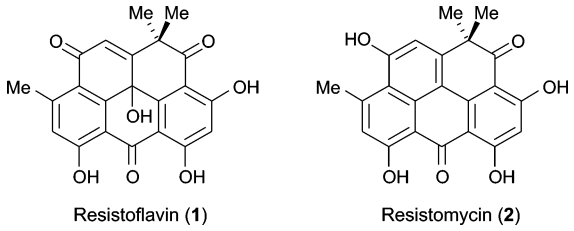

Figure 1. Structures of pentacyclic polyketides produced by *S. resistomycificus*.

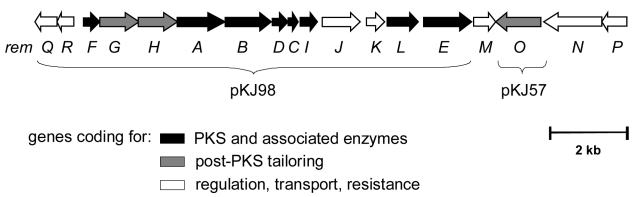

Figure 2. Organization of the *rem* gene locus. Deduced gene functions: RemA−C, min PKS; RemD, PPTase; RemE, MCAT; RemF,I,L, cyclases; RemG,H, methyl transferases; RemJ, kinase; RemK, unknown; RemM,P−R, regulators; RemN, efflux protein; RemO, oxygenase.

After the first discovery of **1** from the culture of an unidentified Actinomycete by Eckardt and co-workers in 1970,[15−17] it was reisolated together with its *O*-methyl derivative from various terrestrial and marine-derived *Streptomyces* species, including *Streptomyces griseoflavus* and *Streptomyces resistomycificus*.[18−20] Isotope labeling studies by Höfle and Wolf clearly established a polyketide origin of **1**.[19] The structure of **1** suggests that this chiral compound is a derivative of the flat, achiral polyphenol resistomycin (**2**). However, neither the exact biosynthetic pathway to the optically active polyphenol nor its absolute configuration has been established to date.

Here we disclose the role of a monooxygenase, RemO, in an unprecedented central, nonperipheral hydroxylation of the planar pentacyclic resistomycin ring system leading to a pseudo-boat-shaped molecule. In addition to *remO* deletion and complementation experiments, we reconstitute the biotransformation in vitro. Furthermore, we disclose the stereochemical course of the oxygenation by comparison of the circular dichroism (CD) spectrum obtained experimentally with the spectra quantum chemically predicted for each of the two possible enantiomers.

Results and Discussion

In the course of our molecular studies on the biosynthesis of resistomycin (*rem*), we noted that downstream of the *rem* locus encoding polyketide formation (*remA−L*), a second operon is located, which features a putative oxygenase gene, *remO* (Figure 2).[5] The deduced gene product shows the highest similarity/identity scores to FAD-dependent monooxygenases from *Nitrobacter hamburgensis* (48/63, EAN59431) and *Agrobacterium tumefaciens* (48/66, AAL43591). RPS-BLAST of the deduced amino acid sequence revealed an FAD binding region (pfam01494) at the *N*-terminus of RemO and a conserved monooxygenase region (pfam01360) at its *C*-terminus. In the fermentation broths of both *S. resistomycificus* and a *Streptomyces lividans* TK23 transformant bearing cosmid pKJ05, **1** was detected by HPLC/MS, albeit only in low amounts of 0.5−5.0 mg L^{-1} (Figure 3c,d). To establish the function of *remO*, the *rem* gene cluster lacking the second operon was subcloned and expressed in a heterologous host (*S. lividans* TK23). An 11.9 kb *Sna*BI/*Eco*RV fragment containing the gene cassette *remQ−E* was excised from pKJ05, subcloned, and ligated into the *Swa*I site of the *E. coli−Streptomyces* shuttle vector pKJ01. The resulting plasmid (pKJ98, Figure 2) was introduced into the expression host *S. lividans* TK23 by PEG-mediated protoplast transformation. A selected positive transformant (*S. lividans* TK23/pKJ98) was cultivated on R5 plates supplemented with thiostrepton.

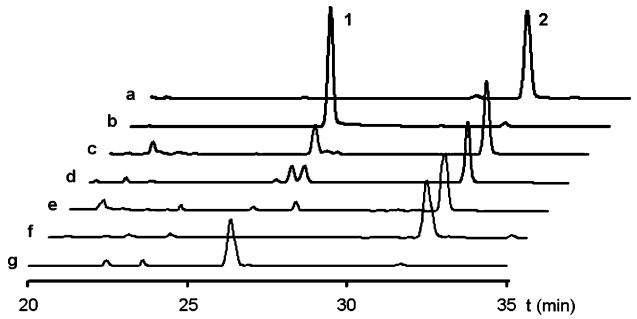

Figure 3. HPLC profiles of extracts and references: (a) reference of **2**, (b) reference of **1**, (c) *S. resistomycificus*, (d) *S. lividans* TK23/pKJ05, (e) *S. lividans* TK23/pKJ98, (f) *S. lividans* TK23/pWHM4* + **2**, cell-free extract, (g) *S. lividans* TK23/pKJ57 + **2**, cell-free extract.

The metabolic profile was monitored by HPLC and mass spectrometry using authentic samples as references. While resistomycin was clearly produced by the transformant, resistoflavin was not detectable (Figure 3e). This demonstrates that the absent genes *remM−P* are not required for resistomycin biosynthesis, and suggested that they are involved in the formation of **1**. The requirement for *remO* for the biosynthesis of **1** was proven by subsequent complementation and biotransformation studies. First, a 1.4 kb genomic region containing the entire *remO* gene together with its ribosome binding site was amplified by PCR using primers KJrem05 and KJrem06 for introducing flanking *Bam*HI and *Eco*RI sites and was subcloned into pGem for sequencing. The 1.4 kb *Bam*HI/*Eco*RI fragment was then cloned into the respective sites in pWHM4* downstream of the constitutive *ermE* promoter, yielding expression plasmid pKJ57. We expected that higher titers of RemO would increase the amount of resistoflavin produced. Surprisingly, coexpression of *remO* with the *remA−L* cassette as well as introduction of the plasmid pKJ57 into the wild-type producer *S. resistomycificus* did not give clear results. Also feeding **2** to a strain expressing *remO* (*S. lividans* TK23/pKJ57) was unsatisfactory, as only partial conversion was observed. We then noted that **1** is readily degraded under fermentation conditions to give **2**. Thus, we aimed at in vitro biotransformations using heterologously produced RemO. Initially *remO* was cloned into expression vectors pRSET and pMalc2x for overexpression of the fusion proteins in *E. coli*. Production of His_6-tagged RemO in *E. coli* BL21 yielded an insoluble enzyme preparation only. By contrast, the MalE−RemO fusion protein was obtained as a soluble fraction (Figure S1 in the Supporting Information) and could be purified using an amylase column. The protein fraction was subjected to a tryptic fingerprint and MALDI-TOF

(15) Eckardt, K.; Bradler, G.; Fritzsche, H.; Tresselt, D. *Z. Chem.* **1970**, *10*, 221.
(16) Eckardt, K.; Fritzsche, H.; Tresselt, D. *Tetrahedron* **1970**, *26*, 5875−5883.
(17) Eckardt, K.; Bradler, G.; Tresselt, D.; Fritzsche, H. *Adv. Antimicrob. Antineoplast. Chemother., Proc. Int. Congr. Chemother., 7th, 1971 (1972)* **1972**, *1*, 1025−1027.
(18) Kock, I.; Maskey, R. P.; Biabani, M. A. F.; Helmke, E.; Laatsch, H. *J. Antibiot.* **2005**, *58*, 530−534.
(19) Höfle, G.; Wolf, H. *Liebigs Ann. Chem.* **1983**, 835−843.
(20) Gorajana, A.; Kurada, B. V. V. S. N.; Peela, S.; Jangam, P.; Vinjamuri, S.; Poluri, E.; Zeeck, A. *J. Antibiot.* **2005**, *58*, 526−529.

analysis, which confirmed the identity of RemO as well as the deduced amino acid sequence from the *remO* gene. Unfortunately, the MalE−RemO fusion protein was not capable of hydroxylating **2**, which may be rationalized by the blockage of the FAD binding site by the maltose binding protein portion (see Figure S2 in the Supporting Information). Cleavage of the maltose binding protein was hampered by the presence of an additional factor Xa cleavage site within the RemO sequence. We thus focused on RemO produced by a *Streptomyces* host. The best results were obtained by a cell-free extract of RemO producing *S. lividans* TK23/pKJ57, obtained by ultrasonication of harvested mycelium. Compound **2** was quantitatively transformed into **1** in PBS buffer using the supernatant of the disintegrate supplemented with FAD and NADH (Figure 3g). The negative control, a cell-free extract of a strain containing the empty vector only, was not capable of this biotransformation, clearly confirming the functional proof of RemO (Figure 3f).

Our in vitro results unequivocally demonstrate that **1** originates from a central enzymatic hydroxylation of **2**. In analogy to other FAD-dependent phenolic hydroxylases,[21,22] we propose that the distal oxygen of flavin C4a-hydroperoxide (FADH−OOH)[23] functions as an electrophile attacking the central carbon of the discoid **2**. However, it should be emphasized that RemO differs from all other known polyketide-modifying oxygenases, which exclusively functionalize the periphery of polyphenolic ring systems. Considering the pseudosymmetric structure of **2**, we were particularly interested in gaining insight into the stereochemical course of the reaction. We thus aimed at assigning the absolute configuration of **1**, which had not been determined to date. Due to the unprecedented structure of resistoflavin (**1**), which does not permit empirical comparison of its CD spectrum with that of any other chiral compound of known configuration, the CD spectra for each of the two possible enantiomers of **1** were predicted by quantum chemical calculations and then compared with the experimental one. Arbitrarily starting with the *R*-enantiomer of **1**, a conformational analysis was carried out at both the semiempirical (AM1)[24] and the DFT (RI-BLYP/SVP)[25−27] levels. The AM1-based computations revealed that the three "outer", phenolic hydroxy functions adopt only one energetically preferable orientation, with strong hydrogen bonds (d_{H-O} = ca. 1.98 Å) to the adjacent respective carbonyl groups, while the inner/interior, bisbenzylic hydroxy group was found to have three possible alignments toward the available carbonyl groups, all being at the same distance. For ring II (for ring numbering see Figure 4) the AM1 calculations predicted two conformations: an energetically favored pseudo-twist-boat geometry with the keto group lying in the plane of the phenyl ring V and, in the case of the central hydroxy group being oriented toward the carbonyl function, a pseudoboat array with the carbonyl group being directed above the plane of ring V. The four conformers thus obtained were further optimized using density functional theory in combination with the resolution-of-identity approximation (RI-BLYP/SVP).[25−27] In this case, no minimum corresponding to the pseudoboat conformation was found, thus diminishing the number of conformers for the subsequent CD calculations to three geometries (Figure 4).

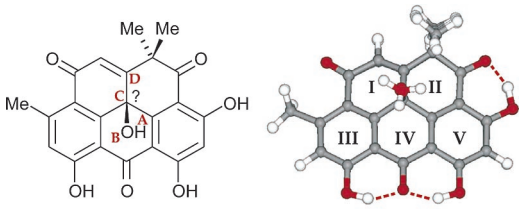

	θ_{ABCD}	$\Delta\Delta H_f$
conf1	63.47	0
conf2	177.31	0.88
conf3	-91.8	2.85

Figure 4. Results of the AM1/BLYP(SVP)-based conformational analysis of **1**: superposition of the three minimum geometries of **1** differing in the orientation of the inner hydroxy group (arbitrarily for the enantiomer with the OH group above the plane, i.e., with *R*-configuration).

The CD and UV spectra of these conformers were calculated by using the semiempirical CNDO/S[28−31] approach and the time-dependent DFT (TDDFT) method using Becke's hybrid exchange-correlation B3LYP[32,33] functional and a TZVP[34] basis set (triple-ζ valence basis set including polarization functions). Overall theoretical spectra were then obtained by adding the single spectra thus calculated, in a Boltzmann-weighted way, i.e., according to the heats of formation of the respective conformer.

Combining high accuracy with computational efficiency, time-dependent DFT CD calculations have recently become an important tool for the assignment of the absolute configuration of small- and medium-sized molecules.[35−37] In the present paper the results of the semiempirical CNDO/S calculations are therefore not considered extensively, while the TDDFT-computed data will be discussed in more detail.

The experimental CD spectrum of **1** appears highly complex, and although it showed a significant resemblance to the CNDO/S-based CD spectrum simulated for the *R*-enantiomer of **1**, some of the experimental features were not reproduced correctly. In detail, a broad band with a positive Cotton effect near 400 nm and a strongly negative band observed at 198 nm were not simulated by the calculations, and the weak peaks at 260 and 275 nm were even predicted with opposite signs (Figure 5).

Therefore, the molecule was submitted to further calculations at a higher level of theory by using the time-dependent DFT method. The CD and UV spectra calculated for the three minima

(21) Entsch, B.; Van Berkel, W. J. H. *FASEB J.* **1995**, *9*, 476−483.
(22) Palfey, B. A.; Massey, V. In *Comprehensive Biological Catalysis, Vol. III/Radical Reactions and Oxidation/Reduction*; Michael, S., Ed.; Academic Press: San Diego, CA, 1998; pp 83−153.
(23) Palfey, B. A.; Ballou, D. P.; Massey, V. In *Active Oxygen: Reactive Oxygen in Biochemistry*; Valentine, J. S., Foote, C. S., Greenberg, A., Liebman, J. F., Eds.; Chapman & Hall: Glasgow, Scotland, 1995; pp 37−83.
(24) Dewar, M. J. S.; Zoebisch, E. G.; Healy, E.; Stewart, J. J. P. *J. Am. Chem. Soc.* **1985**, *107*, 3902−3909.
(25) Bauernschmitt, R.; Häser, M.; Treutler, O.; Ahlrichs, R. *Chem. Phys. Lett.* **1997**, *264*, 573−578.
(26) Lee, C.; Yang, W.; Parr, R. G. *Phys. Rev. B* **1988**, *37*, 785−789.
(27) Schäfer, A.; Horn, H.; Ahlrichs, R. *J. Chem. Phys.* **1992**, *97*, 2571−2577.
(28) Del Bene, J.; Jaffé, H. H. *J. Chem. Phys.* **1968**, *48*, 1807−1813.
(29) Bringmann, G.; Mühlbacher, J.; Reichert, M.; Dreyer, M.; Kolz, J.; Speicher, A. *J. Am. Chem. Soc.* **2004**, *126*, 9283−9290.
(30) Pérez, A.; Ramírez-Durón, R.; Piñeyro-López, A.; Waksman, N.; Reichert, M.; Bringmann, G. *Tetrahedron* **2004**, *60*, 8547−8552.
(31) Bringmann, G.; Gulden, K.-P.; Busemann, S. *Tetrahedron* **2003**, *59*, 1245−1253.
(32) Becke, A. D. *J. Chem. Phys.* **1993**, *98*, 1372−1377.
(33) Becke, A. D. *J. Chem. Phys.* **1993**, *98*, 5648−5652.
(34) Schäfer, A.; Huber, C.; Ahlrichs, R. *J. Chem. Phys.* **1994**, *100*, 5829−5835.
(35) Furche, F.; Ahlrichs, R.; Wachsmann, C.; Weber, E.; Sobanski, A.; Vögtle, F.; Grimme, S. *J. Am. Chem. Soc.* **2000**, *122*, 1717−1724.
(36) Voloshina, E.; Fleischhauer, J.; Kraft, P. *Helv. Chim. Acta* **2005**, *88*, 194−209.
(37) Wang, Y.; Raabe, G.; Repges, C.; Fleischhauer, J. *Int. J. Quantum Chem.* **2003**, *93*, 265−270.

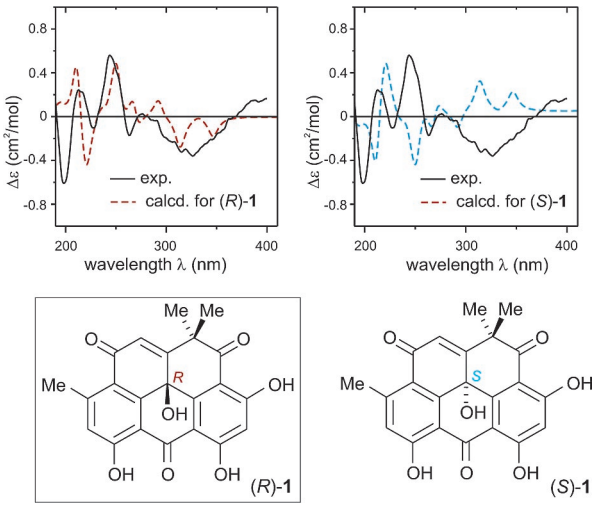

Figure 5. Comparison of the experimental CD spectrum of **1** (in methanol) with the CNDO/S-based CD curves predicted for its two enantiomers, (*R*)-**1** and (*S*)-**1**. By "UV correction",[38] the calculated spectra were red-shifted by 0.34 eV (i.e., 18 nm).

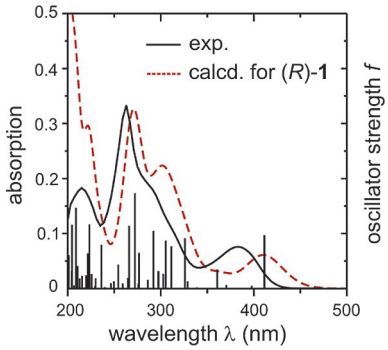

Figure 6. Experimental and B3LYP-predicted UV spectra of **1**. The red dotted curve presents a Boltzmann-weighted UV profile. The sticks indicate the positions and the oscillator strengths *f* of the calculated states of the global minimum of **1** (*conf1*).

of **1** were now found to be very similar, differing only in the positions of the respective transitions. The most important transitions with the corresponding oscillator, *f*, and rotatory, *R*, strengths of the three conformers are listed in the Supporting Information (see Tables S1−S3).

The calculations showed that the overall UV spectrum is red-shifted in comparison to the experimental one by 0.20 eV (i.e., 12 nm), with respect to the most intensive UV band, which could be due to a systematic underestimation of the excitation energies in TDDFT (B3LYP)[39] (Figure 6). The low-intensity band with the maximum observed at 383 nm could be correlated with the HOMO−LUMO (102−103) excitation at $\lambda_{calcd} = 411$ nm (Table S1 and Figure 7). This excitation gives rise to the first Cotton effect in the calculated CD spectrum, which has a positive sign as in the experimental CD spectrum (Figure 8). An assignment of the most intense band observed at 264 nm with a shoulder (near 288 nm) was complicated by the presence of many excited states with high *f* values predicted in the region of 326−266 nm; however, all of them are characterized by the dominating transitions to the molecular orbital 105, which is a

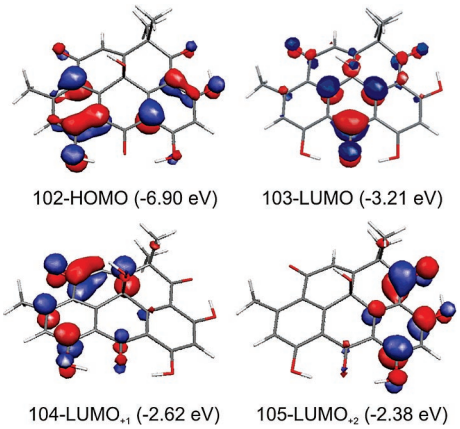

Figure 7. Highest occupied molecular orbital (102) and the lowest three unoccupied molecular orbitals (103−105).

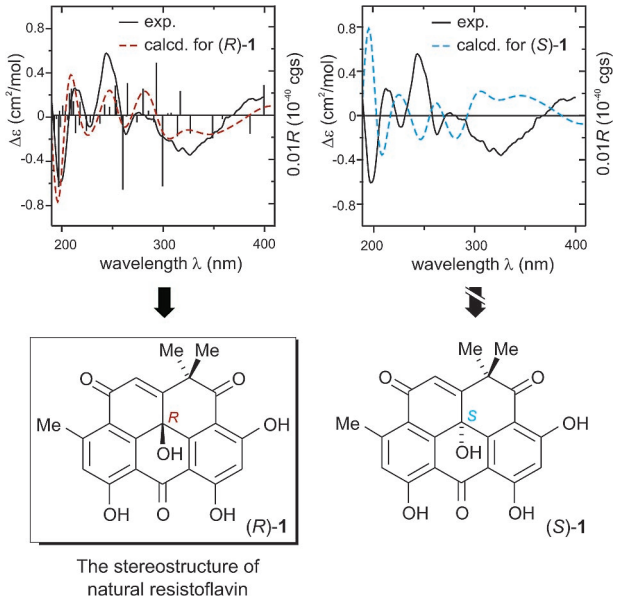

Figure 8. Comparison of the experimental CD spectrum of **1** with the computationally predicted ones (B3LYP/TZVP). The red and blue dotted curves represent Boltzmann-weighted CD spectra with a blue shift of 0.20 eV (i.e., 12 nm). The sticks indicate the shifted positions and the rotatory strengths *R* of the calculated states of the global minimum.

π*-type orbital with the main contributions on the carbonyl group of ring II and two hydroxy functions of ring V (Figure 7).

In the experimental CD spectrum a broad negative band near 325 nm was correlated with the calculated transitions at 361, 339, 326, and 311 nm, representing mainly the excitations to MOs 103 (LUMO) and 104 (LUMO + 1), the latter one being a π* orbital with large contributions of the functionalities in the "western" part of molecule **1** (Figures 7 and 8). The next low-intensity CD band observed at 275 nm was assigned to the calculated one at 292 nm, although the predicted intensity is too high. This absorption predominantly arises from a $\pi_{ring}-\pi_{C=O,C-OH}$ excitation occurring from molecular orbital 101 to the LUMO + 2 (105) (see also Figure S3 in the Supporting Information). The negative Cotton effect at 260 nm was correlated with the calculated one at 272 nm, which has a multiconfiguration character (Table S1). The following four experimental bands were well reproduced by the calculations, too, although their unambiguous assignment to particular calculated states was not possible.

(38) Bringmann, G.; Busemann, S. In *Natural Product Analysis*; Schreier, P., Herderich, M., Humpf, H. U., Schwab, W., Eds.; Vieweg: Wiesbaden, Germany, 1998; pp 195−212.
(39) Bauernschmitt, R.; Ahlrichs, R. *Chem. Phys. Lett.* **1996**, *256*, 454−464.

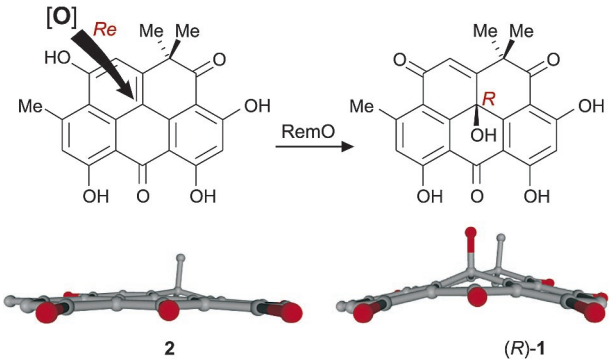

Figure 9. Stereochemical course of the RemO-catalyzed hydroxylation of **2**.

The B3LYP/TZVP-calculated CD spectrum for (*R*)-**1**, finally, showed a very good agreement with the experimental curve, reproducing all features. Accordingly, the spectrum predicted for (*S*)-**1** nicely displayed an opposite behavior, thus clearly assigning the absolute configuration of naturally occurring resistoflavin (**1**) as *R*. See Figure 9.

Conclusions

In summary, by in vivo and in vitro experiments we have disclosed the function of RemO as an FAD-dependent monooxygenase involved in resistoflavin biosynthesis. The successful in vitro biotransformation assay using heterologously expressed *remO* revealed that the pseudo-boat-shaped pentacyclic ring system of resistoflavin (**1**) is derived from a stereospecific interior, nonperipheral hydroxylation of the planar polyphenol resistomycin (**2**). In addition, we were able to establish the absolute configuration of **1** and thus the stereochemical course of this rare enzymatic reaction by extensive computational methods. Comparison of the CD spectra calculated for (*R*)-**1** and (*S*)-**1** with the experimental CD spectrum of resistoflavin unequivocally established its *R*-configuration. Consequently, the enzyme-catalyzed hydroxylation takes place from the *Re*-face of **2** with loss of planarity/aromaticity of ring I. While other oxygenases involved in polyketide tailoring functionalize the periphery of polyphenols,[40] RemO is unique in its ability to catalyze a central, nonperipheral hydroxylation of a fused ring system. Thus, RemO is an important new addition to the present chemoenzymatic toolbox. Further biochemical studies are in progress, which will reveal factors controlling substrate binding and the detailed mechanism of stereospecific oxygen transfer.

Experimental Section

General Procedures. Flash chromatography was performed using a CombiFlash RETRIEVE system by Teledyne Isco, Inc., Lincoln, NE, with 120 g Redi*Sep* silica columns. Preparative HPLC was performed on a Shimadzu HPLC system with a UV detector using a Waters Spherisorb S5ODS2 250 × 20 column (flow rate 18 mL min^{-1}). Analytical HPLC was carried out on a Shimadzu HPLC system consisting of an autosampler, high-pressure pumps, a column oven, and a DAD. HPLC conditions: C18 column (Nucleosil 100, 5 μm, 125 × 3 mm) and gradient elution (1:99 MeCN/0.1% TFA/H_2O in 30 min to 100:0 MeCN/0.1% TFA/H_2O, 100% MeCN for 10 min), flow rate 1 mL min^{-1}.

DNA manipulation, transformation procedures, and fermentation were performed according to standard protocols.[38] All plasmids were introduced into expression host *S. lividans* TK23 or *S. resistomycificus* by PEG-mediated protoplast transformation.

Isolation and Purification of Resistoflavin (1). Cultures of *S. resistomycificus* were fermented in M10 medium (with a total volume 10 L) for 4 d at 28 °C with shaking at 140 rpm. The crude extract obtained from exhaustive ethyl acetate extraction of mycelium and broth was purified by open-column flash chromatography on silica using a $CHCl_3$/MeOH gradient as the eluent (flow rate 30 mL min^{-1}). Fractions containing resistoflavin were further purified by preparative HPLC (isocratic 60% MeCN/40% 0.1% TFA, flow rate 18 mL min^{-1}, UV detection at 268 nm). Final purification was achieved by size-exclusion chromatography using a Sephadex LH-20 column with $CHCl_3$/MeOH (1:1) as eluent. Yield: 25 mg of pure **1**. The identity of resistoflavin was confirmed by NMR and HPLC/MS analysis using an authentic sample generously provided by Prof. H. Laatsch, Göttingen, Germany.

Heterologous Expression of *rem* Biosynthesis Genes. The truncated *rem* gene cluster *remQ*−*E* was generated by excision of an 11.9 kb *Sna*BI/*Eco*RV fragment from pKJ05 subcloned and ligated into the *Swa*I site of pKJ01,[5] yielding pKJ98. *remO* was amplified by PCR using primers KJrem05 (CG*G GAT CC*G TCA TCC CGC TCA TTC, *Bam*HI site italic) and KJrem06 (CG*G AAT TC*G GTG GTC GAC ACC ATC T, *Eco*RI site italic) using the cosmid clone pKJ05 as template and cloned into pGem-T Easy for subcloning and sequencing. The 1.4 kb *Bam*HI/*Eco*RI fragment was then ligated into the corresponding sites of pWHM4* downstream of the constitutive *ermE* promotors. The resulting plasmid pKJ57 was introduced into *S. lividans* TK23 by PEG-mediated protoplast transformation. The resulting transformant was selected and cultured on 2CM medium supplemented with thiostrepton for harvesting spores. In analogy the negative control *S. lividans* TK23/pWHM4* was generated. For feeding experiments, resistomycin (each 0.5 mg, dissolved in DMSO) was added to 50 mL cultures and grown for 4 d at 30 °C at 200 rpm. Crude ethyl acetate extracts were dried, the solvent was evaporated, and the residue was dissolved in methanol (0.5 mL) for HPLC/MS monitoring (see below).

Overexpression of RemO/MalE−RemO in *E. coli* and MALDI-TOF Analysis. ORF *remO* was amplified by PCR using primers RemOfw (AAG ACC GAG GCC CAG) and RemOrv (TCA GGA CAC GTG CTC AGG AC) using cosmid clone pKJ05 as template and cloned into pMOS*Blue* for sequencing prior to ligation into pRSET and pMALc2x, respectively. PCR reaction was performed using TripleMaster polymerase mix as described by the manufacturer (Eppendorf). For expression of RemO, *E. coli* BL21 (DE3), transformed with the appropriate vector, was precultured overnight. A 500 μL portion of an overnight culture was inoculated into 50 mL of LB containing ampicillin. The culture was grown at 37 °C to an OD_{600} of 0.5, and then expression of protein was induced by the addition of IPTG. Cell growth continued for 4 h at 30 °C.

In-gel digestion of MalE−RemO was performed as described previously.[41] The tryptic peptides were recovered from the resulting particles with 20 μL of 50% acetonitrile/0.1% TFA (1:1), assisted by ultrasonication. For MALDI-TOF-MS analysis, 3 μL of the sample was mixed with 3 μL of matrix [saturated α-cyano-4-hydroxycinnamic acid in acetonitrile/0.1% TFA (3:7)].

In Vitro Hydroxylation of 2 and Monitoring of 1 Production. To prepare the protein crude extracts containing RemO, *S. lividans* TK23/pKJ57 was cultivated in R5 medium (100 mL) with thiostrepton (50 μg mL^{-1}) at 30 °C for 6 d. The cultured medium was centrifuged

(40) For other natural products originating from a similar—yet peripheral—oxygenation, see: (a) Abe, N.; Arakawa, T.; Yamamoto, K.; Hirota, A. *Biosci., Biotechnol., Biochem.* **2002**, *66*, 2090−2099. (b) Bringmann, G.; Lang, G.; Gulder, T. A. M.; Tsuruta, H.; Mühlbacher, J.; Maksimenka, K.; Steffens, S.; Schaumann, K.; Stöhr, R.; Wiese, J.; Imhoff, J. F.; Peroviæ-Ottstadt, S.; Boreiko, O.; Müller, W. E. G. *Tetrahedron* **2005**, *61*, 7252−7265. (c) Qhotsokoane-Lusunzi, M. A.; Karuso, P. *Aust. J. Chem.* **2001**, *54*, 427−430. (d) Wube, A. A.; Bucar, F.; Asres, K.; Gibbons, S.; Rattray, L.; Croft, S. L. *Phytother. Res.* **2005**, *19*, 472−476.

(41) Shevchenko, A.; Wilm, M.; Vorm, O.; Mann, M. *Anal. Chem.* **1996**, *68*, 850−858.

(6000 rpm for 10 min at 4 °C), and harvested cells were resuspended in 20 mL of an ice-cold PBS buffer (pH 7.0). The suspension was sonicated in an ice bath (ultrasonic generator, Bandelin Sonoplus HD2200; sonotrode, MS73; conditions, 9 × 1 min sonication at 50% duty cycle and 1 min interval, cool at 10 °C). The supernatant obtained by centrifugation (8600 rpm for 20 min at 4 °C) was kept in an ice bath until use in the activity assay. Resistomycin (100 μg, 1 mg mL^{-1} in DMSO) was added to the crude extract solution (4.0 mL), and then the reaction mixture was incubated at 30 °C with shaking overnight. The resulting mixture was extracted three times with EtOAc (4.0 mL), and after the removal of solvent in vacuo, 100 μL of methanol was added.

Enzyme activity was determined by the HPLC analysis using a Nucleosil 100/5 C18 (3 × 125 mm) reversed-phase column. The following gradient was applied at a flow rate of 1.0 mL min^{-1}: linear gradient from 99.5:0.5 (water containing 0.1% TFA/acetonitrile) to 1:99 in 40 min. The UV detection was carried out at 268 nm.

Computational Methods. The conformational analysis of resistoflavin (**1**) was performed on a Linux AMD MP 2800+ workstation using the semiempirical AM1[24] method as implemented in the program package Gaussian 98.[42] The final optimization was carried out with the DFT/RI-BLYP/SVP[25−27] approach within the TURBOMOLE[43] suite of programs. The wave functions of the ground and excited states were obtained by semiempirical CNDO/S-CI[29] computations with a CI expansion including 576 occupied configurations and the ground state determinant and by a time-dependent DFT approach, with 80 excited states being lowest in energy, which were calculated using the B3LYP[32,33] functional and a TZVP[34] basis set. In both approaches the oscillator and rotatory strengths were computed using the dipole-length formalism.[44] The rotatory and oscillator strengths calculated for the single conformers were added according to the Boltzmann statistic. The spectra were then simulated as sums of Gaussian functions centered at the wavelengths of the corresponding electronic transitions and multiplied by the respective overall rotatory or oscillator strengths. For both UV and CD spectra, an empirically chosen exponential half-width of 0.1 eV was used. Molecular orbital plots were generated by the MOLEKEL program.[45]

Acknowledgment. This work has been funded by DFG Grant HE3469/1 (for C.H.) and within the DFG priority program SPP1152: "Evolution of Metabolic Diversity" Br699/9-2 (for G.B.). We thank Mandy Sitz for assistance, Prof. H. Laatsch, University of Göttingen, for an authentic sample of resistoflavin, A. Perner and Dr. O. Scheibner for HPLC/MS measurements, and R. Winkler for MALDI-TOF measurements.

Supporting Information Available: SDS−PAGE for MalE−RemO expression experiments, amino acid sequence and model for RemO, plot of HOMOs of **1**, tables of the results based on (TD)B3LYP/TZVP (*Conf1*−*Conf3* geometries), and complete refs 42 and 43. This material is available free of charge via the Internet at http://pubs.acs.org.

JA064550U

(42) Frisch, M. J.; et al. *Gaussian 98*, Revision A.7; Gaussian, Inc.: Pittsburgh, PA, 1998.
(43) Ahlrichs, R.; et al. *TURBOMOLE 5.6*; Universität Karlsruhe: Karlsruhe, Germany, 2002.
(44) Harris, R. A. *J. Chem. Phys.* **1969**, *50*, 3947−3951.
(45) Flükiger, P.; Lüthi, H. P.; Portmann, S.; Weber, J.; *MOLEKEL 4.3*; Swiss Center for Scientific Computing: Manno, Switzerland, 2000−2002.